GIS and Geostatistical Analysis of the La Plata Mining District

David S. Schiowitz[1], W. Scott White[2], and Jeffrey A. Cary[3]

[1]GIS/CAD Specialist
Bikis Water Consultants, LLC
555 RiverGate Lane, Suite B4-82
Durango, CO 81301
970-385-2340
david@bikiswater.com

[2]Associate Professor
Department of Geosciences – Fort Lewis College
1000 Rim Drive
Durango, CO 81301
970-247-7475
white_s@fortlewis.edu

[3]Visiting Instructor
Department of Geosciences – Fort Lewis College
1000 Rim Drive
Durango, CO 81301
970-247-7620
cary_j@fortlewis.edu

ABSTRACT

The La Plata mining district is located in southwestern Colorado, and contains numerous gold, silver, and copper deposits. Geologic and structural data for the district was obtained from georeferencing and digitizing an historic geologic map. New stream sediment samples were collected at 41 locations throughout the area, and analyzed for metal concentrations. Using ArcGIS's surface hydrologic modeling tools, individual watersheds were delineated upstream for each sediment sample location. A geodatabase has been created consisting of geologic formations and structures, veins, rock ages, historic mines, and geochemical anomalies associated with the 41 watersheds. The Spatial Analyst extension was used to analyze the data to aid in visualization and quantification of the relationships among geology, structure, and geochemistry. The results provide greater insight into regional geochemical domains of mineralization and in the modeling of spatial associations of known ore deposits within the mining district.

Introduction

The objective of this project was to build a spatial database of structural, lithological, and geochemical data, so that a spatial model for gold exploration could be created. This model was created using the Fuzzy Logic Method developed by Graeme Bonham-Carter of the Geologic Survey of Canada, and Gary Reins of the USGS. Gold geochemical data was collected in the La Plata Mountains of southwestern Colorado, during the summer and fall months of 2007. This mountain range has been the focus of numerous mineral exploration and extraction projects for over 100 years. To find possible sites for new mineral deposits, diverse information from geological, geochemical, remote sensing data (including satellite images and aerial photographs), and topographical data, needed to be managed and integrated to define target areas, and this was accomplished using GIS, specifically ArcGIS 9.2 (ArcInfo). The main reason for using GIS during mineral exploration is to predict the approximate positions of new mineral deposits by creating a spatial model of the area of interest. Previous researchers (e.g. Cross, 1899, and Eckel, 1949) mapped the surface geology and structures of the La Plata mining district. This research mapped, analyzed and discussed different lithologies, minerals, ore deposits and structures in the La Plata Mountains area and produced a 1:31,680 scale geologic map of the district. The National Uranium Resource Evaluation (NURE) program (1974-1984) collected regional geochemical stream sediment samples of the western United States, including four samples taken from the La Plata River in southwestern Colorado. These studies concluded that there were precious metals in the La Plata Mountains. However, no detailed spatial analysis has correlated geochemical anomalies, surface geology and structural features in the region. Since the advance of GIS technology, the geology of the La Plata Mountains has not been studied in a regional context; therefore, by integrating different datasets into a GIS, a spatial model of ore prediction has been created for the mining district.

Location

The La Plata Mountains are located approximately 12 miles northwest of Durango in southwestern Colorado (Figure 1). The mountains rise rapidly on the west, south, and southeast from the generally level Colorado Plateau. They lie about 20 miles southwest of the main San Juan Mountain front.

The main peaks lie within a 9-mile ring that is centered near the mouth of Tirbircio Creek in the La Plata River valley (Figure 2). The highest elevation is Hesperus Peak, which stands 13,225 ft. above sea level and the lowest point has an elevation of 7,250 ft. The area is very rugged and steep, with 79% of the area above 9,000 feet and almost 19% above 11,000 feet (Eckel, 1949).

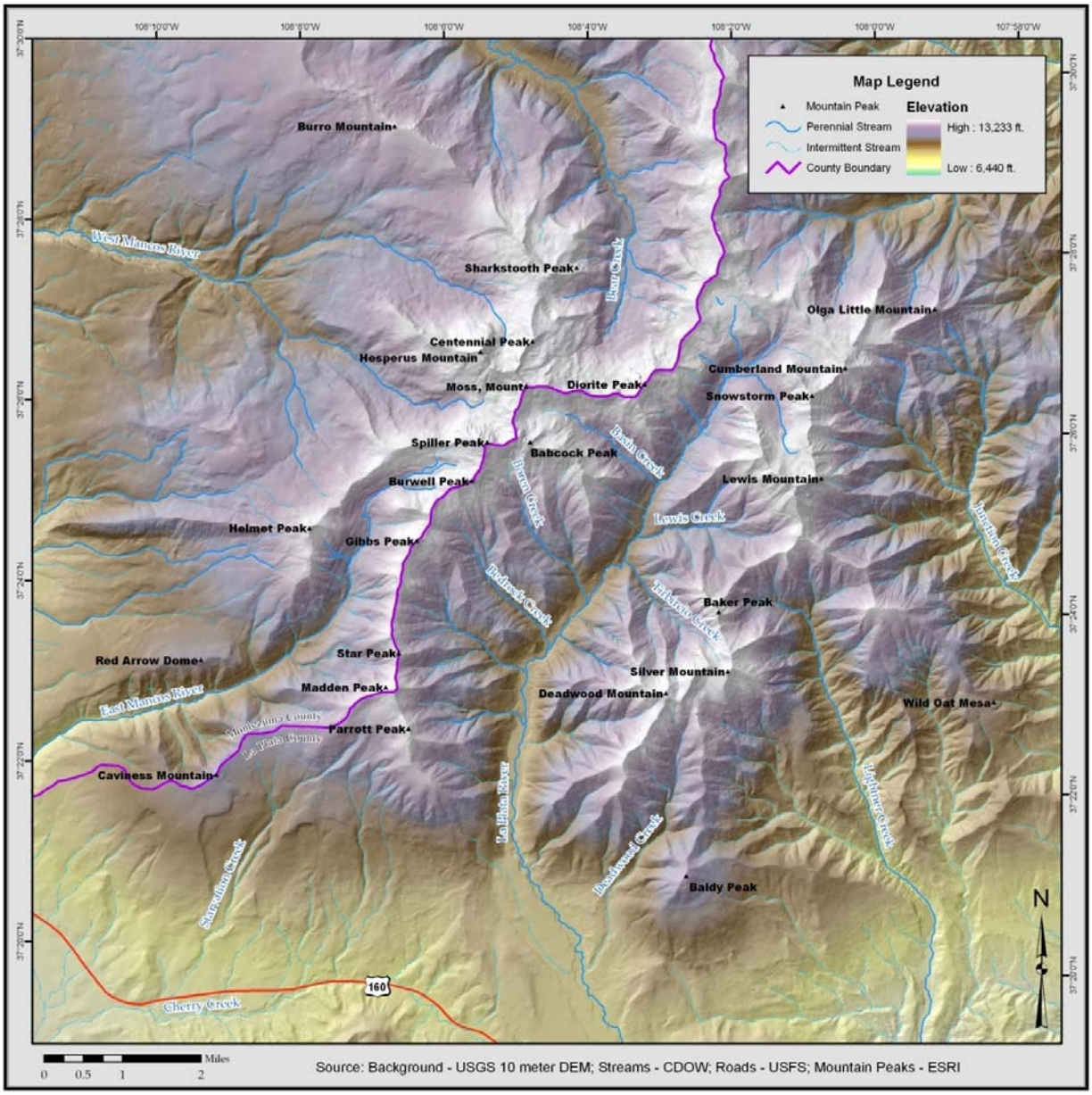

Figure 1. Location of the La Plata Mountains in relation to the southwest United States.

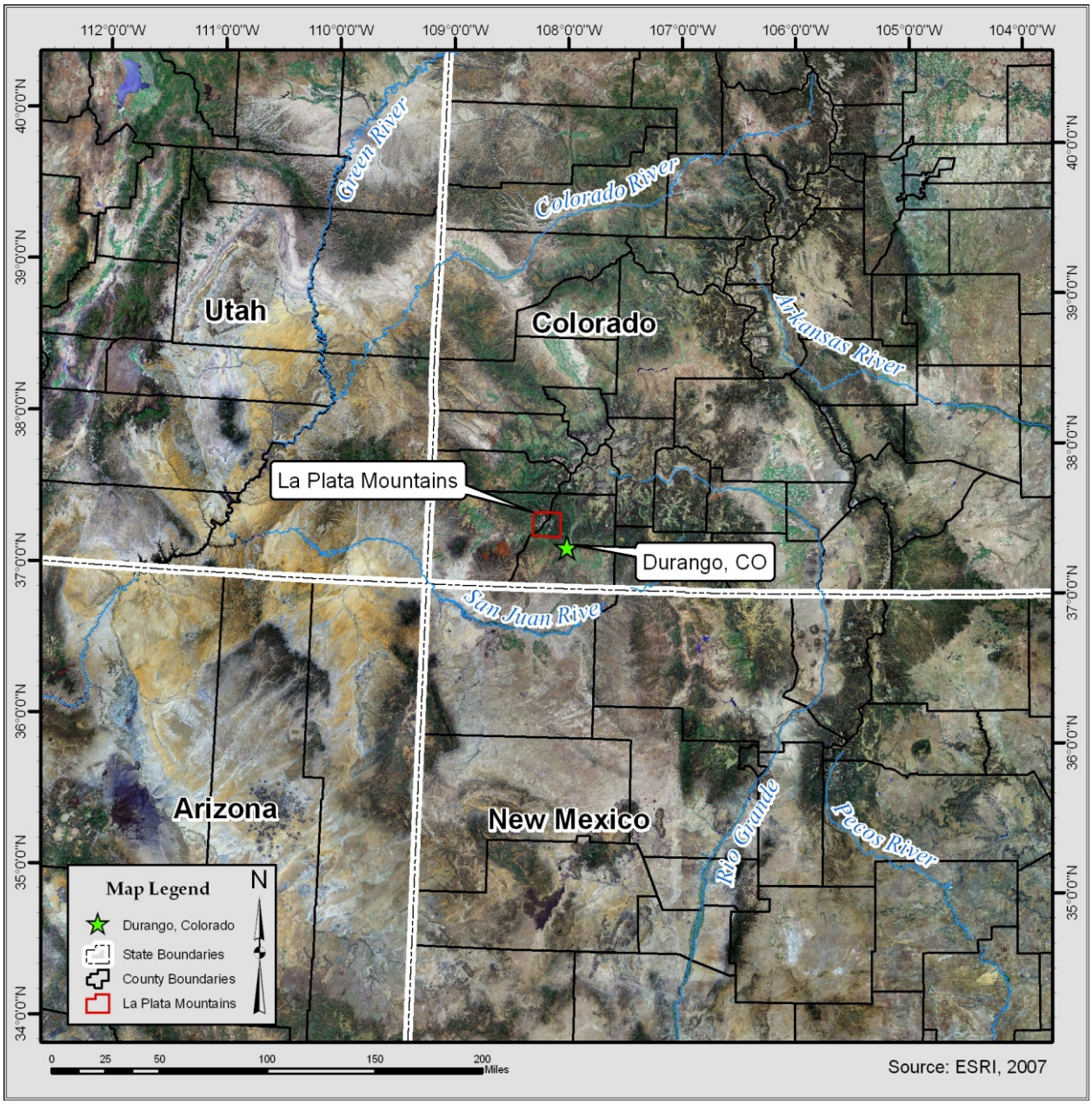

Figure 2. Overview map of the La Plata Mountains with a USGS 10 meter DEM and a shaded relief background. Major streams, creeks, roads, peaks and county boundaries are shown.

Overview of the Economic Geology of the La Plata Mountains

The La Plata mining district is situated at the southwestern end of the Colorado mineral belt. The belt was the site of abundant igneous activity, including the formation of hydrothermal ore deposits during the Tertiary. The La Plata district resides in the center of a dissected dome that was formed by the intrusion of stocks, sills, dikes, and laccoliths into Paleozoic and Mesozoic sedimentary rocks (Saunders and May, 1986).

The exposed sedimentary rocks range in age from the Pennsylvanian Hermosa Formation to the Upper Cretaceous Dakota Sandstone and Mancos Shale. These predominantly clastic sedimentary rocks dip away from the central higher areas. The dome has approximately 10,000 ft. of structural relief and is asymmetrical due to a horseshoe-shaped fold that opens to the south (Trauger, 1968). This fold caused some sedimentary rocks to dip, as steeply as 75°; however, on both sides of the fold, the majority of dips are relatively flat (Saunders and May, 1986). Faulting with large amounts of displacement is common on the outer parts of the dome, and in the central area of the dome, there are many small fractures and faults (Eckel, 1949).

The igneous rocks of the La Plata Mountains are all intrusive and are of Late Cretaceous or Tertiary age. They differ extensively in composition and in form, and are grouped into two general types: porphyritic and nonporphyritic. Porphyry sills are very abundant and range in thickness from a few inches to 300 feet or more (Eckel, 1936). The sills are concentrated around the center of the uplift and most are squeezed between the beds of sedimentary rocks. Porphyry dikes have varying thicknesses and are common throughout the district. The stocks, dikes, and sills have similar composition and texture, and it has been suggested that they all formed contemporaneously. These porphyritic rocks are most likely responsible for forming the structural dome of the La Plata Mountains (Eckel, 1936). The nonporphyritic rocks are generally younger than the porphyritic rocks and consist of syenite, monzonite and diorite intrusions. These rocks occur as irregular stocks with many associated dikes (Eckel, 1936).

The intrusion of nonporphyritic rocks caused widespread contact metamorphism and hydrothermal alteration of the country rocks in the central portion of the La Plata district. The majority of the sedimentary rocks in the central part of the district have been strongly metamorphosed. After metamorphism, widespread introduction of pyrite took place. This metamorphic event is associated with the nonporphyritic rocks, because the porphyries are altered and sedimentary rocks in contact with the porphyries are unaltered (Eckel 1949).

The formation of the structural dome, along with associated fault and fractures, is believed to have occurred at the same time as the porphyry intrusion. The dome precedes the intrusion of the granular stocks and regional metamorphism. Faults are believed to be the main controlling structures of ore deposits in the La Plata district, but it is unknown how these faults relate to hydrothermal alteration. There are many faults and fractures throughout the district that have been mineralized. They are mostly normal faults, but some mineralized reverse faults do exist. Displacement ranges from inches to hundreds of feet. These faults show a small trend

toward a radial array, with regard to the dome. Most of these ore-bearing faults trend northeast to east and are less than a mile long. The majority only extend a few hundred feet. The longer fault zones consist of a series of overlapping fractures. These structures are the main mode of fluid movement during mineralization and make up the majority of ore deposits in the area (Trauger, 1968). There are two large breccia zones in the central part of the district. In these zones, the rocks are brecciated and sheared along fractures and minor faults that trend northeast. Pyrite and chalcopyrite are widespread in these zones and are very common near fractures. Some of these fractures have workable gold deposits. It is suggested that there was upward extension in the basement rock that allowed ore solutions to gain access to the higher rocks, thus creating valuable gold and silver deposits (Eckel, 1949).

The La Plata mining district has a variety of ore deposits, which include contact-metamorphic deposits, gold-bearing pyrite deposits, replacement bodies, breccia deposits, mixed sulfide with gold and silver, chalcocite veins, ruby silver veins, and telluride veins. These deposits all share characteristics of alkaline rock-hosted porphyry Cu-Au metal deposits (Werle and others, 1984). Almost 95% of the production has been gold and silver that is associated with gold-bearing telluride ores (Eckel, 1949).

Exploration Model

Using previous observations (Eckel, 1949; Saunders and May, 1986; Trauger, 1968; Werle and others, 1984) and generic models developed by the British Columbia Geological Survey (Panteleyev, 1995), an exploration model was created. The model illustrates the major features associated with gold mineralization (Table 1). This exploration model will help in the data extraction process used to create the ore prediction map.

Table 1 Exploration Model

Commodity of Interest	Gold
Generic Model Types	Polymetallics Veins/Alkalic Intrusion
Favorable Host Rocks	Wanakah Formation, Entrada Sandstone, and Junction Creek Sandstone, hornfels aureole
Favorable Structures	Quartz veins, vein stockworks, breccias, and second order structures adjacent to major faults
Geochemical Signature	Au, As, Ag, Ba, Hg, Sb, Se, Pb, Zn, Te
Ore Minerals	Au-Ag tellurides and free gold

Spatial Model Creation

The processes of creating a spatial model of potential ore deposits includes four main steps: (1) assembling a diverse spatial database of relevant features, (2) extracting and compiling predictive evidence for a specific ore deposit model, (3) investigating each dataset in order to generalize and/or classify it, and (4) joining the classified datasets to predict potential mineral deposits (Sawatzky and others, 2007).

To conceptualize the data, the Fuzzy Logic Method was chosen because it is suitable to use whenever one has to deal with ambiguity, vagueness and uncertainty in creating a conceptual model of observed phenomena (Burrough, 1998). In classical GIS modeling, the process involves converting multiclass maps into a binary predication pattern. This assumes a crisp boundary between favorable and unfavorable areas, but in reality this boundary is imprecise, and thus fuzzy. Therefore, fuzzy logic is the logic behind approximate reasoning, instead of exact reasoning. Fuzzy logic allows one to introduce subjectivity and vagueness in a mathematical computer analysis. It does this by assigning a fuzzy membership to each dataset (usually a raster grid). The fuzzy membership is a user-defined value between 0 and 1 that represents its association with a particular model (0 having no membership and 1 having full membership). Values are chosen to reflect the degree of membership to a fuzzy set.

The Fuzzy Logic Method involves two main steps. First, raster datasets are converted into fuzzy evidence maps. This is accomplished using functions that transform raw data into a fuzzy set with values between 1 and 0. Next, the fuzzy evidence maps are combined using fuzzy operators to create a final favorability map. Depending upon the exploration model, the generalized or "fuzzified" datasets can be combined using one or a combination of the following fuzzy logic combinational operators (Bonham-Carter, 1994):

- ***Fuzzy OR*** is like Boolean *OR* operator (logical union). The output membership values are controlled by the maximum value of input grid. The function is defined as $\mu_{Combination} = \text{Max}\ (\mu_A, \mu_B, \mu_C, \ldots\ldots)$
- ***Fuzzy AND*** is like the Boolean *AND* operator. The output membership values are controlled by the minimum value of the input grid. The function is defined as $\mu_{Combination} = \text{Min}\ (\mu_A, \mu_B, \mu_C, \ldots\ldots)$
- ***Fuzzy algebraic product*** is defined as $\mu_{Combination} = {}^{i=1}\Pi^{n}\ (\mu_i)$; Where μ_i is the fuzzy membership values of ith map and $i= 1,2,3,..n$
  The combined fuzzy membership values tend to be very small due to multiplying effect of several numbers less than 1, thus the effect is decreasing.
- ***Fuzzy algebraic sum*** is complementary to algebraic product and defined as $\mu_{Combination} = 1 - {}_{i=1}\Pi^{n}\ (1 - \mu_i)$; Where μ_i is the fuzzy membership values of ith map and $i= 1,2,3,..n$. The result of this operation is always larger than or equal to largest contributing fuzzy membership value, thus the effect is increasing.

- ***Fuzzy gamma*** operator is defined as $\mu_{Combination}$ = (fuzzy algebraic sum)$^{\gamma}$ * (Fuzzy algebraic product)$^{(1-\gamma)}$
  The γ value is arbitrary and ranges from 0 to 1. When γ is equal to 0 then the combination is the same as the fuzzy algebraic product. When γ is equal to 1 then the combination is the same as the fuzzy algebraic sum.

Step 1. Data Collection

To build a geodatabase that can then be used for mineral potential mapping, several geological, geochemical and historical mine data sets were acquired. Geologic data (including faults, veins, major lithologies, and formation contacts) were obtained by digitizing and georeferencing a historical geologic map produced by Edwin Eckel of the USGS in 1949. After the map was georeferenced, surface geology (contacts and formations), veins and faults were digitized and incorporated into a geodatabase. Surface geology was attributed with a map unit, general rock type and approximate age. The linear features were attributed by type (fault, approximate fault, vein and approximate vein) and azimuth. Azimuth values were determined by a utility included in the Spatial Data Modeller extension (ArcSDM). ArcSDM contains a collection of geoprocessing tools that can be used to predict the occurrence of some type of phenomenon (Sawatzky and others, 2007). ArcSDM is a free extension and can be downloaded at *http://arcscripts.esri.com/details.asp?dbid=15341.*

To define the geochemical provinces of the La Plata Mountains, active stream sediment sampling was selected as an appropriate method because it would give a representation of the geochemistry upstream of the sampling location. A total of 41 active stream sediment samples were collected in the La Plata Mountains (Figure 3) by the primary author of this study during the summer and fall months of 2007. These samples were collected using a miner's pan and a quarter-inch sieve. The samples were analyzed for 69 elements using an ICP-OES (5g, partial acid digestion) from American Assay Laboratories, Inc. (AAL), and gold concentrations were analyzed using a 30 gram fire assay from AAL. Individual watersheds were delineated using each sample location as a pour point/catchment point. Watersheds were created using a processed 10 meter DEM from the USGS. Results from the geochemical analysis were then joined to their respective watershed polygon and loaded into the geodatabase.

Historical mine data were acquired using the USGS Mineral Resources On-Line Spatial Data website (USGS, 2008). Past and present producing gold mines were extracted from the database. These files were then loaded into the geodatabase and were used to evaluate the spatial model (Figure 4).

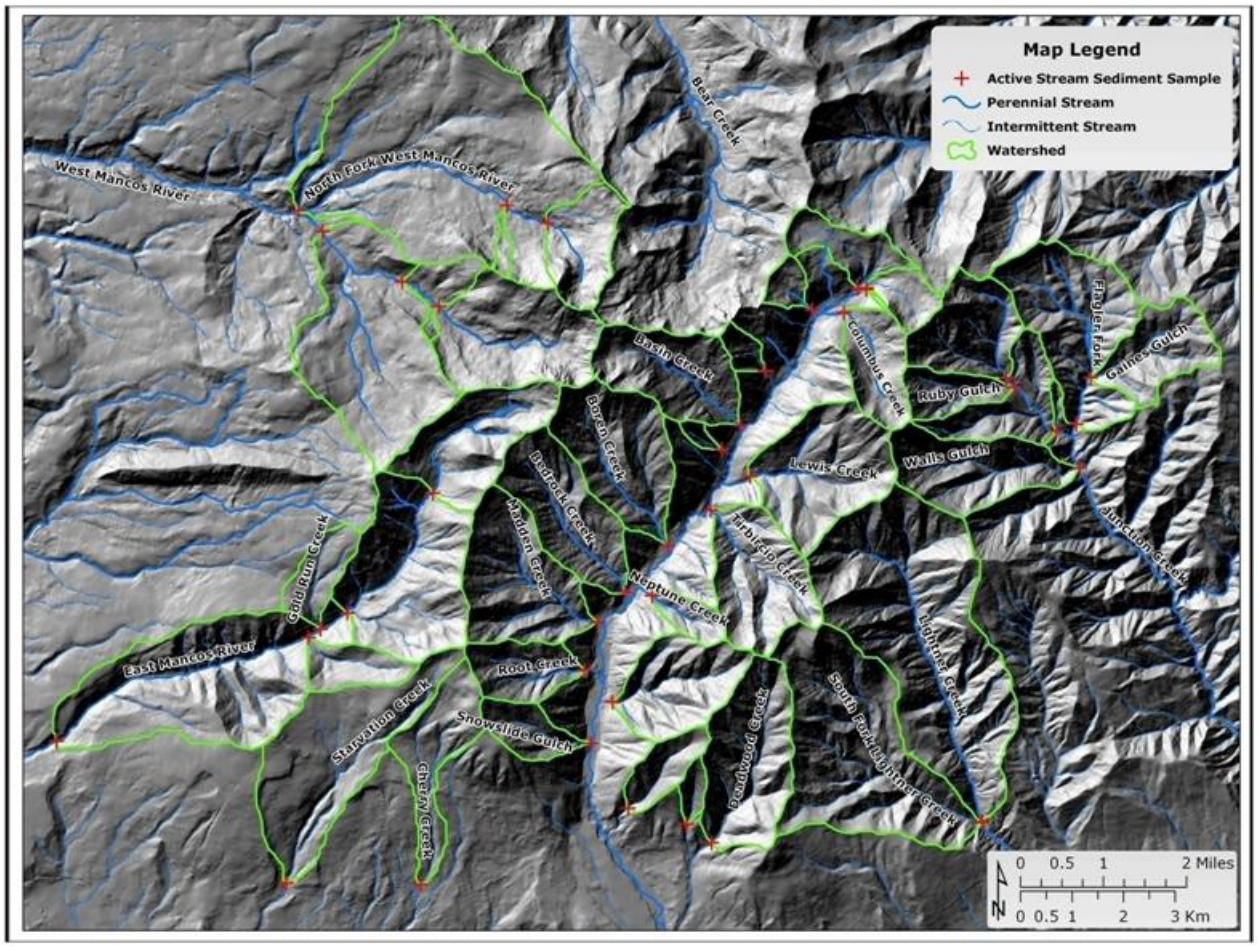

Figure 3. Sample locations map with associated watersheds.

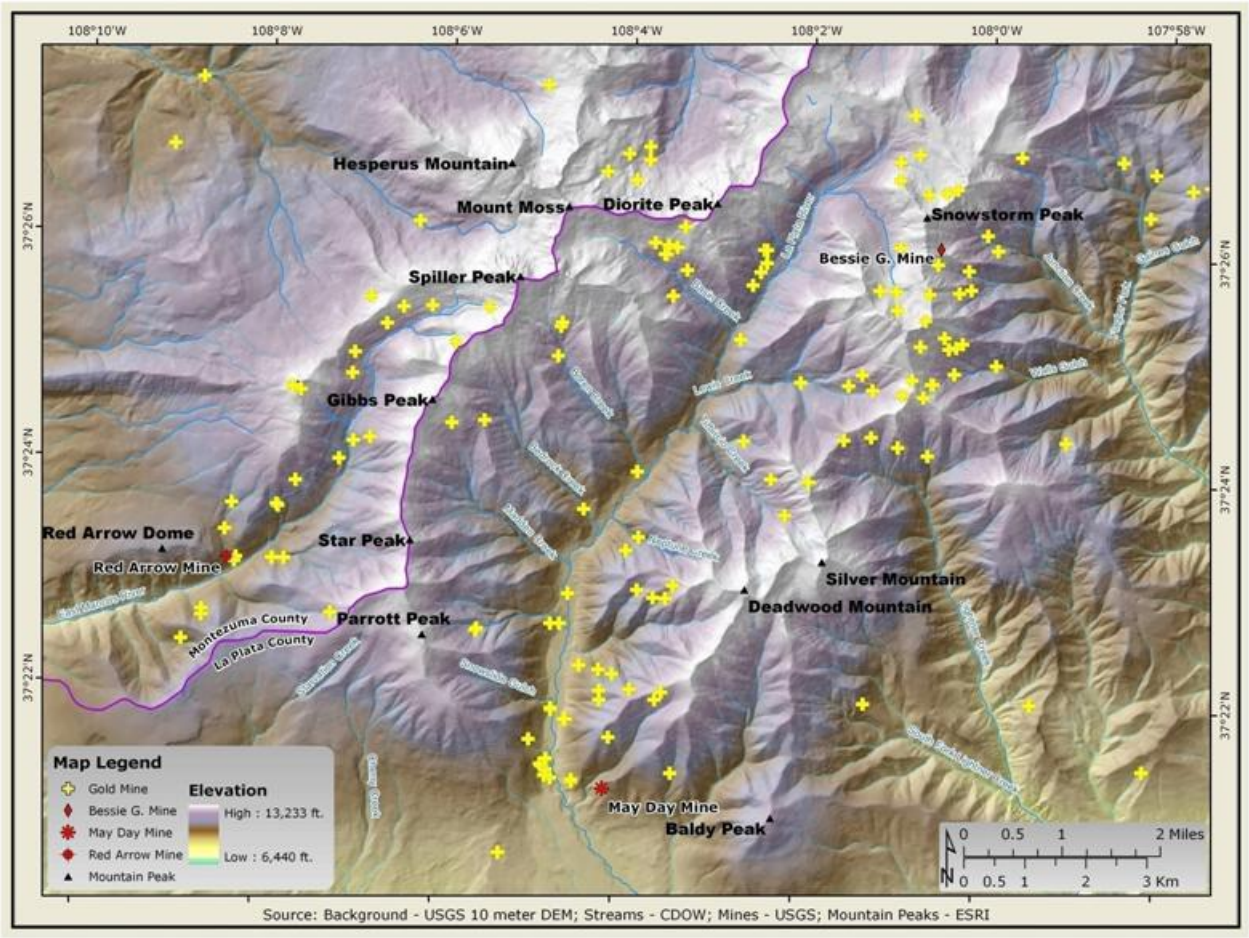

Figure 4. Past and present producing gold mines location map. Three major mines (Red Arrow, May Day, and Bessie G.) are shown in red.

Step 2. Data Extraction

Based on the exploration model (Table 1), pertinent GIS features were extracted from the geodatabase and converted into raster grids using the Spatial Analyst Extension in ArcGIS v.9.2. These layers are summarized in Table 2.

Table 2. Extracted and Created Layers

Raster Grid	Raster Grid Z Values
Formations grid	Categorical data based on Formation type
500 meter buffer from a vein grid	Floating point grid based on distance from linear feature
Linear features density Grid	Floating point grid based on the density of linear features
Igneous 500 meter buffer Grid	Floating point grid with cells based on distance from igneous formations
Watersheds for Au, Ag, As	Integer grid based on each elements' concentration

Formations were converted using the Convert Features to Raster tool in ArcGIS with a cell size of 5 meters. Igneous formations (TKd, TKi, TKmz, TKsp, TKs) were extracted from the raster grid, and using the Straight Line Distance tool, a 500 meter buffer was applied to represent possible contact metamorphic/hornfels aureole zones.

Linear features were converted to raster surfaces in two ways. Veins were converted using the Straight Line Distance tool with a maximum distance of 500 meters and a cell size of 5 meters (Figure 5). This created a raster grid representing the distance from a vein. The second conversion created a density grid of veins and faults. The Kernel Density tool was used with a search radius of 500 meters and units of meters per kilometers squared. The resulting raster (Figure 6) illustrates the vein and fault density in the district.

Geochemical data were extracted using the Convert Features to Raster tool to create raster grids based on each element's (Au, As, Ag) concentration to its respective watershed. Using the Geostatistical Wizard in the Geostatistical Analyst extension, each geochemical dataset was interpolated using ordinary kriging to create a geochemical predication surface. Each surface was created using a spherical model with default lag, sill and nugget values. A smooth searching neighborhood was used with a smooth factor of 0.7, and major semiaxis, and minor semiaxis values of 500 meters. Kriging was used because it provides a powerful interpolation tool to predict geochemical trends in areas that were not analyzed. These interpolated surfaces were then exported as raster grids. Figure 7 shows the geochemical basins map for gold.

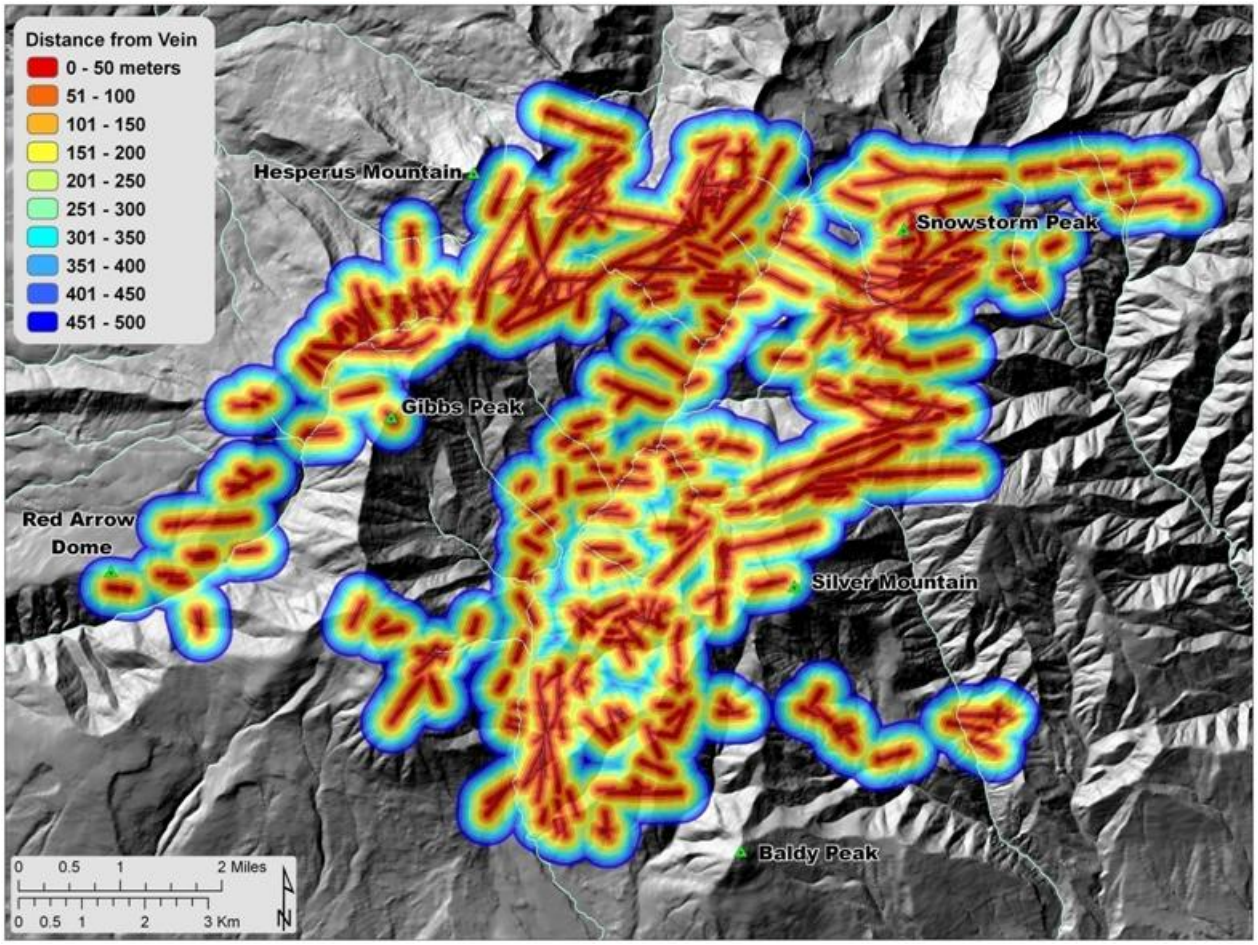

Figure 5. Distance from vein map. Red represents areas closer to a vein and blue represents areas farther from a vein. Maximum distance from a vein is 500 meters (blue).

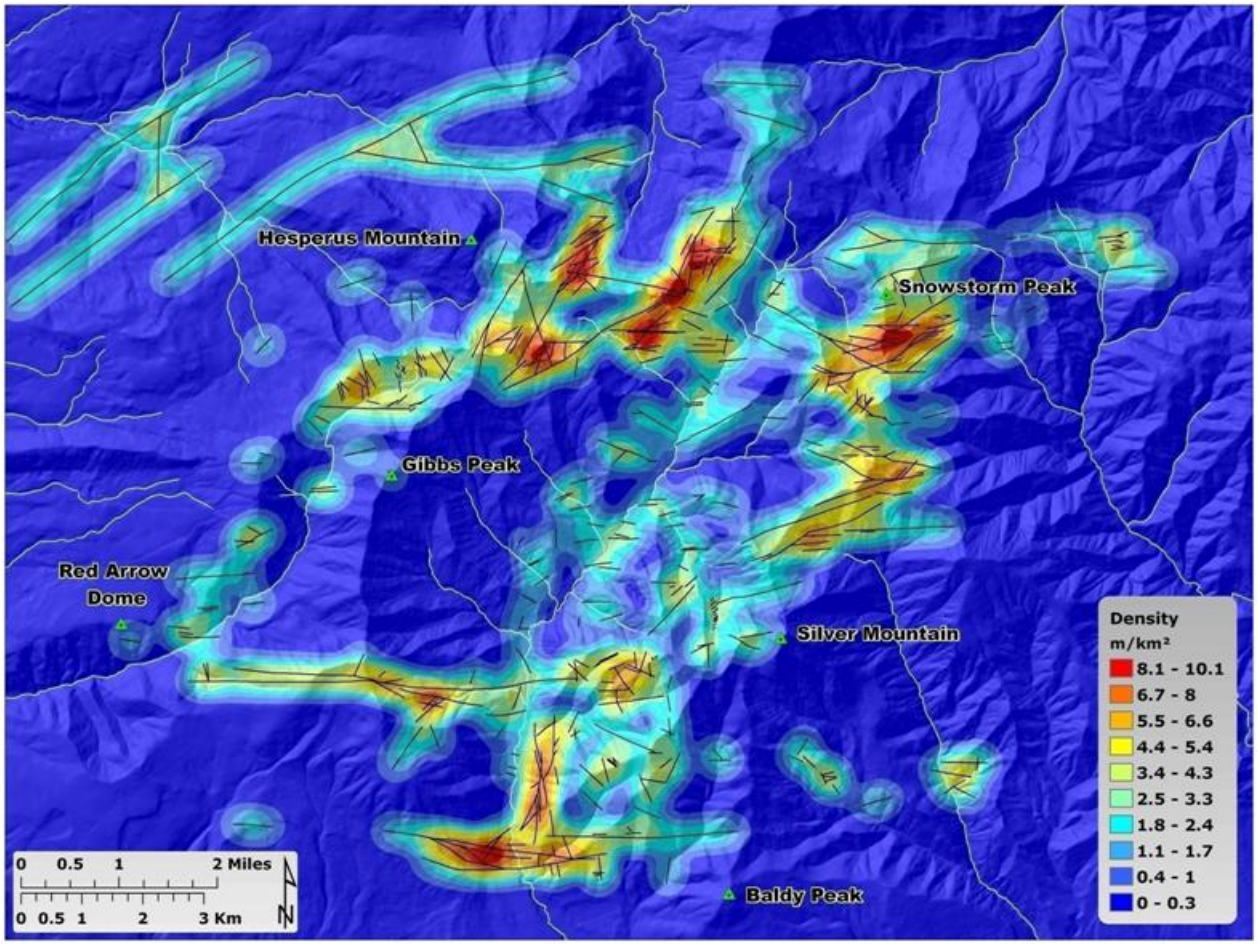

Figure 6. Vein and fault density map overlaid with veins and faults. Areas in red represent regions of high fault/vein density and indicate areas of highly fractured rock.

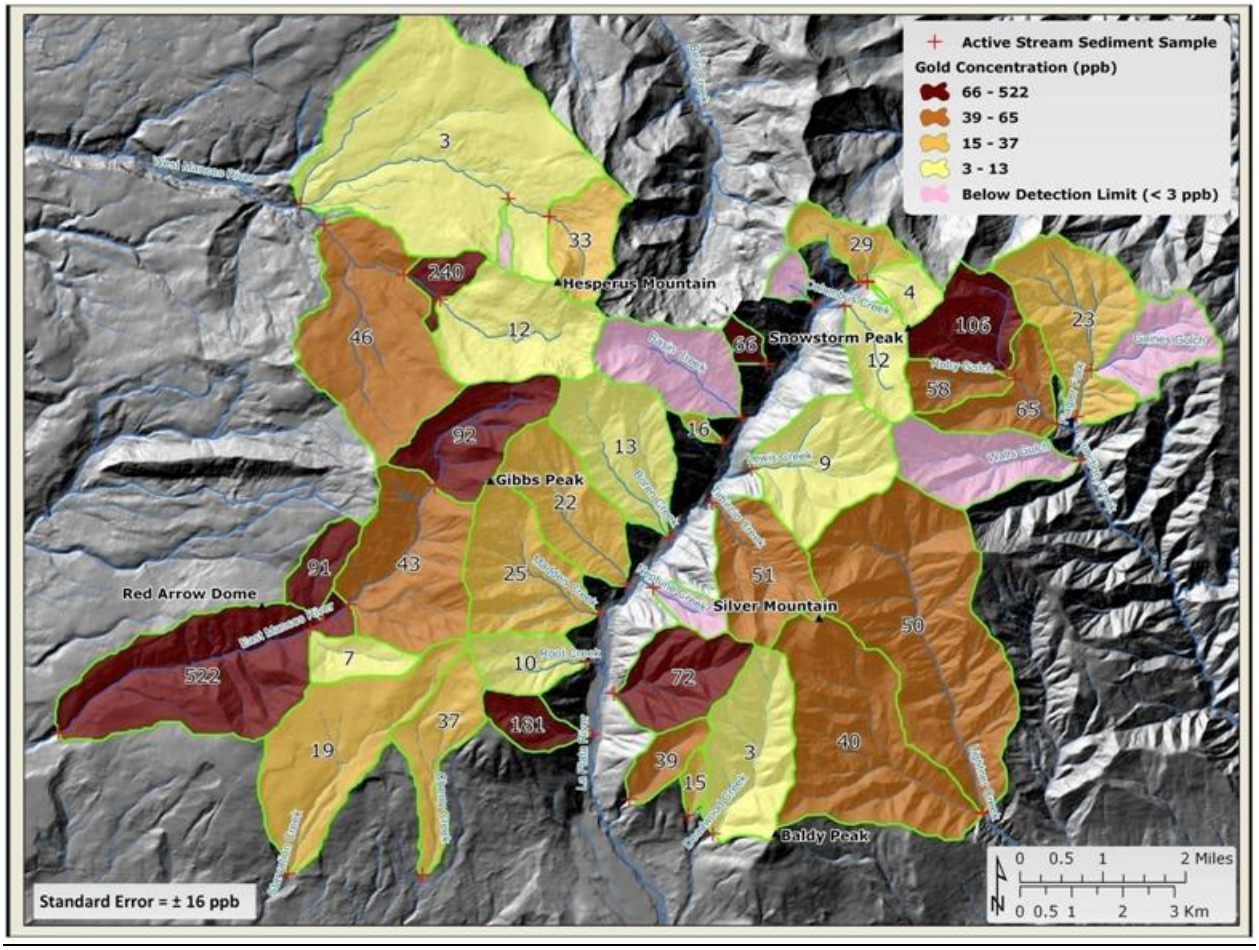

Figure 7. Gold geochemical basins map. Concentrations are shown in ppb.

Step 3. Fuzzification

The Fuzzy Logic Method requires the raster grid to have cell values that range from 0 to 1 depending upon their association with the model. This requires the data to be classified using fuzzy membership functions/tools before it can be combined using fuzzy logic combinational operators. This process involves using the ArcSDM toolkit and the Spatial Analyst extension. To create a prediction surface for possible gold mineralization, the raster grids listed in Table 2 were categorized using the Fuzzy Membership tools provided in the ArcSDM toolkit.

Formations were classified by assigning a score value between 0 and 9 to each formation and then dividing that value by 10. Favorable host rocks (Wanakah Formation, Entrada Sandstone, and Junction Creek Sandstone) were given higher scores, igneous bodies were given middle scores, and unfavorable host rocks were given low values. The resulting membership values are shown in Table 3.

Table 3. Gold Model Formations

Formation	Score	Fuzzy
Wanakah Formation	9	0.9
Entrada Sandstone	8	0.8
Junction Creek Sandstone	8	0.8
Dakota Sandstone	7	0.7
Hermosa Formation	7	0.7
Syenite Intrusion	5	0.5
Diorite Intrusion	5	0.5
Syenite Porphyry	5	0.5
Diorite-Monzonite Porphyry	5	0.5
Monzonite Porphyry	5	0.5
Lamprophyres	5	0.5
Morrison Formation	3	0.3
Cutler Formation	3	0.3
Dolores Formation	2	0.2
Mancos Shale	2	0.2
Landslide deposit	0	0
NoData	0	0

It is assumed that areas closer to veins or igneous formations are more likely to host gold mineralization; therefore, these cells were classified with a higher membership value. The 500 meters from a vein grid was transformed using the Fuzzy Small tool (Equation 1) with a spread of 1 and a midpoint of 200 meters. The 500 meters from an igneous formation grid was transformed using the Fuzzy Small tool with a spread of 2 and a midpoint of 150. The Fuzzy Small tool is based on the small fuzzification algorithm (Equation 1) developed by Tsoukalas and Uhrig (1997). This algorithm transforms small values of an input dataset into larger values of the fuzzy membership dataset. The spread and midpoint parameters are chosen subjectively by the user (Figure 8).

$$\mu(x) = \frac{1}{1+\left(\frac{x}{f_2}\right)^{f_1}}$$

Equation 1. Small fuzzification algorithm, where f_1 is the spread of the transition from a membership value of 1 to 0 and f_2 is the midpoint where the membership value is 0.5 (Tsoukalas and Uhrig, 1997).

The linear feature density grid was classified as shown in Table 4. Areas with greater density were considered to have higher membership values than less dense areas; as a result, the grid was classified by categorizing the grid values into 10 classes using the Natural Breaks method. These classes are represented by the score field in Table 4. The score value was then divided by 11 to create fuzzy membership values.

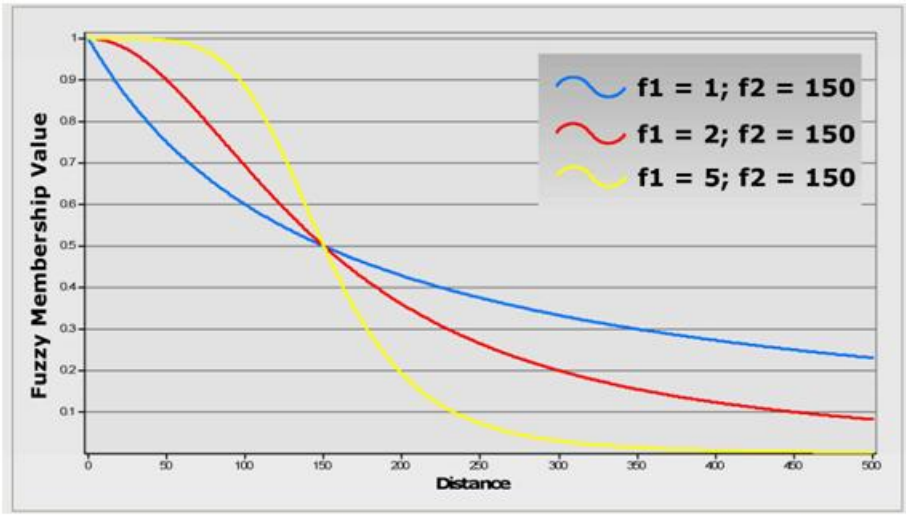

Figure 8. Fuzzy Small algorithm showing different spread values of the igneous 500 meter buffer grid. As the spread values get smaller the longer it takes the fuzzy membership value to reach zero.

Geochemical grids were transformed using the Fuzzy Mean-Standard Deviation Large tool (MS Large) in the ArcSDM toolkit (Equation 2). The MS Large algorithm was developed by Lou and Dimitrakopoulos (2003). The function is like the Fuzzy Small tool with the midpoint and the spread controlled by the mean and standard deviation of the data. The function generates large values for high concentrations and small values for low concentrations. Each geochemical raster (Au, Ag, As) used a mean multiplier of 0.5 and a standard deviation multiplier of 0.5 to generate fuzzy membership rasters. A graph of the gold fuzzy membership function is shown in Figure 9. The mean and standard deviation multiplier values were chosen to account for the large outliers in each of the geochemical datasets.

$$\mu_A(X) = \begin{cases} 1 - \dfrac{bs}{x - am + bs}, & x > am, \\ 0, & \text{otherwise}, \end{cases}$$

Equation 2. Mean-Standard Deviation Large algorithm, where *s* is the standard deviation of the dataset, *m* is the mean, *a* is the multiplier of the mean and *b* is the multiplier of the standard deviation. The user can change the *a* and *b* values to scale the effect of the mean and standard deviation. (Lou and Dimitrakopoulos, 2003).

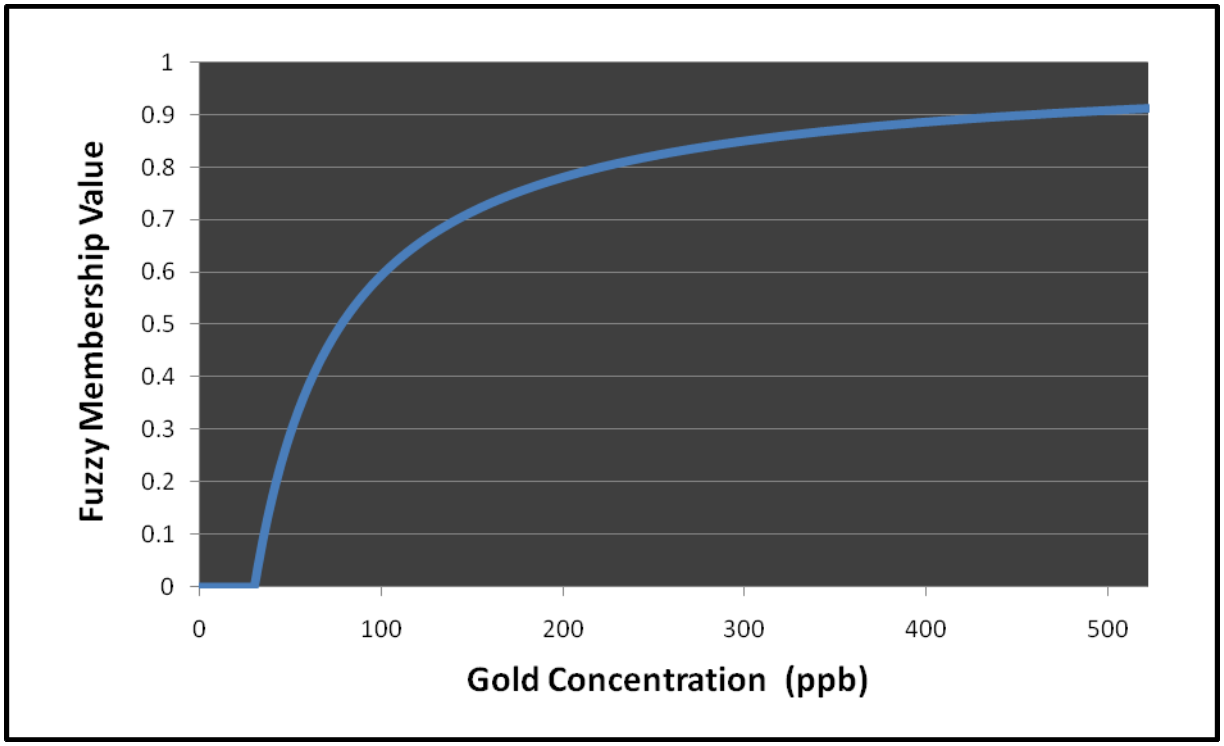

Figure 9. Fuzzy MS large algorithm (Equation 2) using gold concentrations. Fuzzy membership values (y-axis) are plotted against gold concentrations (x-axis). Concentrations less than half of the mean were given membership values of zero while other concentrations were given membership values based on Equation 2.

Step 4. Combining the Data

Conceptual generation of the gold model is shown in Figure 10. The model assumes that each fuzzy membership raster has an influence on the final gold prediction map. Using a ***Fuzzy OR*** operator the gold, arsenic, and silver fuzzy membership grids were combined to create a geochemical evidences grid (Figure 11). The geochemical evidences grid represents the maximum value of each individual geochemical grid. The ***OR*** operator was chosen because any basin with high concentrations of gold, silver or arsenic is a possible indicator of mineralization in its respected basin.

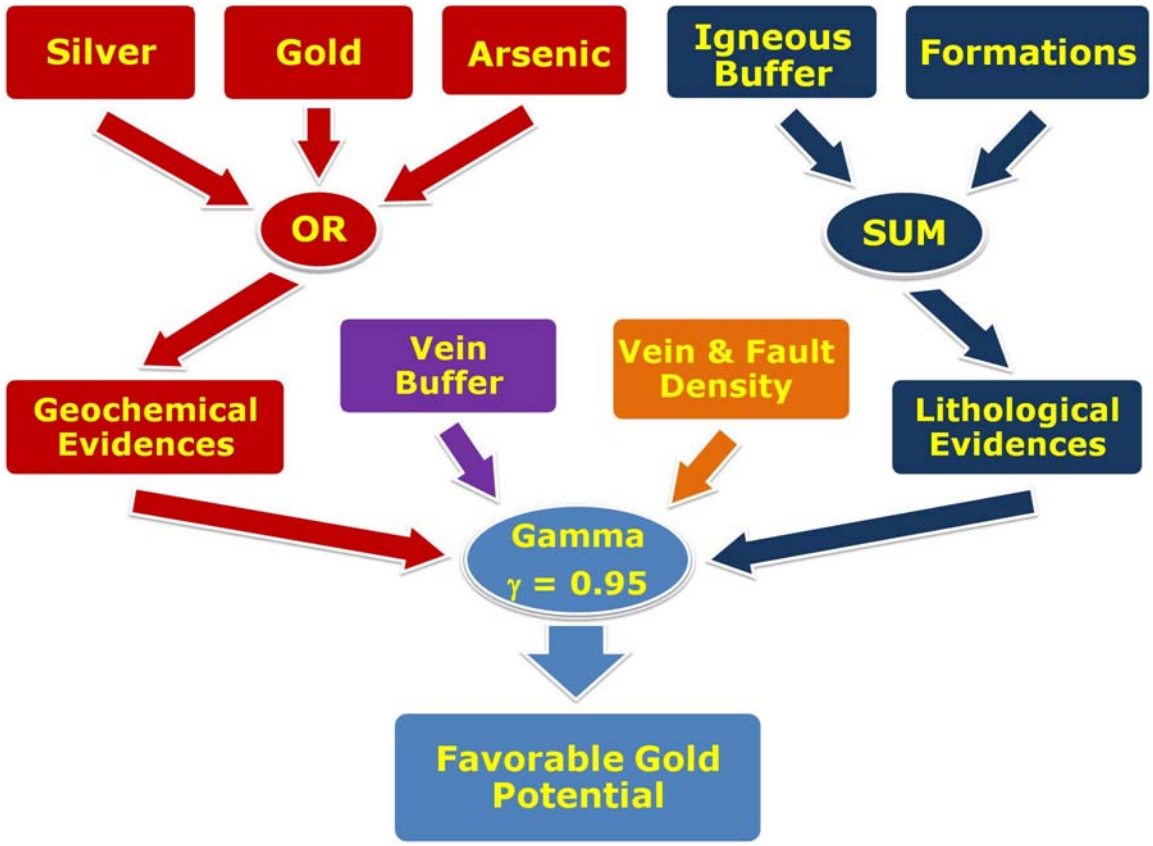

Figure 10. Conceptual model of the different fuzzy membership maps used to create the final gold potential map. Model assumes structures have more influence on the deposition of gold.

Using a ***Fuzzy Sum*** operator, the igneous 500 meter buffer grid was combined to the gold formations grid to create a lithological evidences grid (Figure 12). The **SUM** operator creates a surface that assumes host rocks that are closer to igneous intrusions are more likely to host mineralization than host rocks that are farther away from igneous bodies.

Using a ***Fuzzy Gamma*** operator ($\gamma = 0.95$) the geochemical evidences, lithological evidences, vein buffer and linear feature density grids were combined to create favorable gold potential grid (Figure 13). The **Gamma** operator was used because different gamma values can be chosen to reflect the degree of support that the input maps have on the final potential map. A high gamma value was used because the combination of each one of the evidences in the model has a positive influence on the potential of gold mineralization.

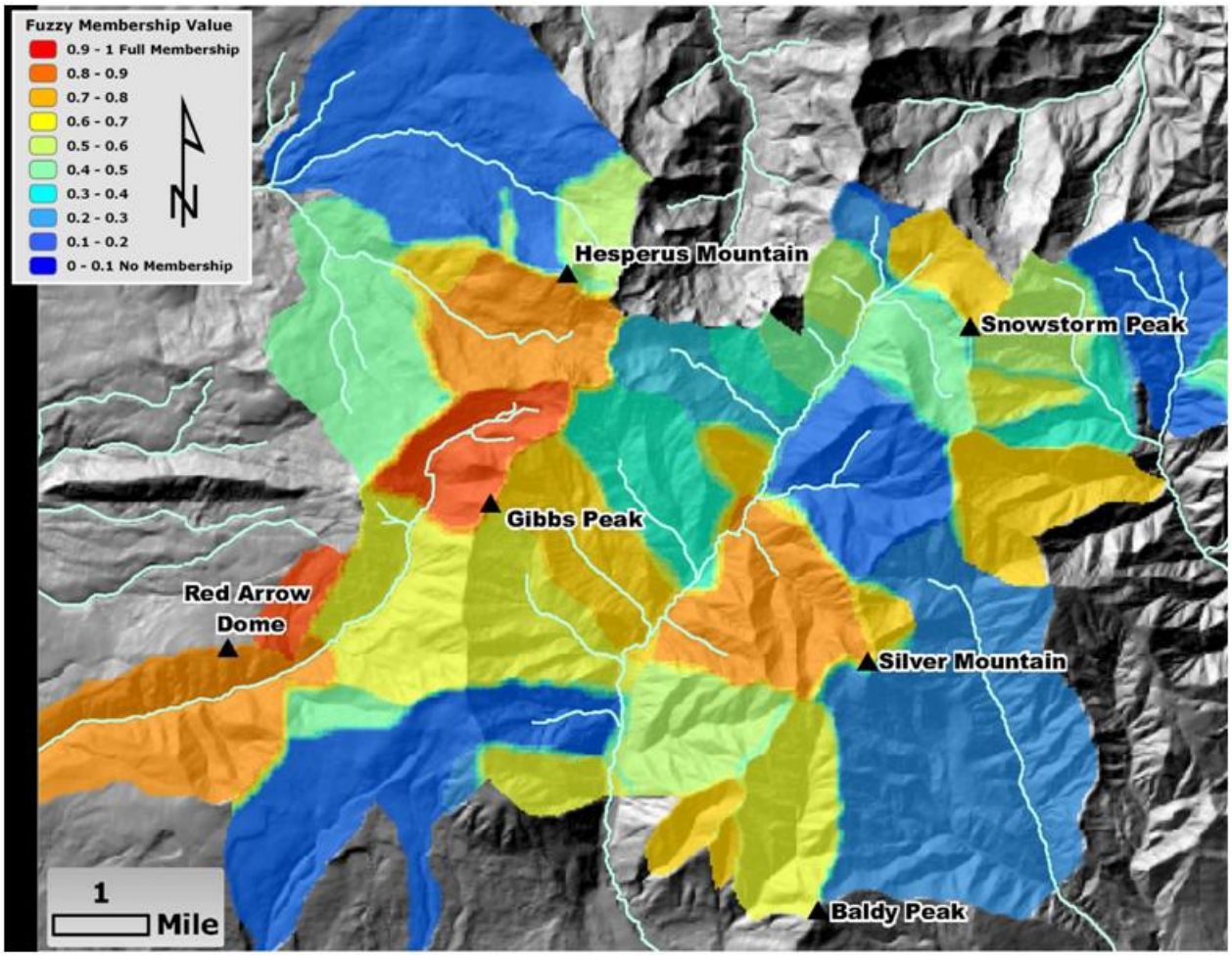

Figure 11. Geochemical evidences map. Areas in red represents areas of high concentrations of gold, silver or arsenic.

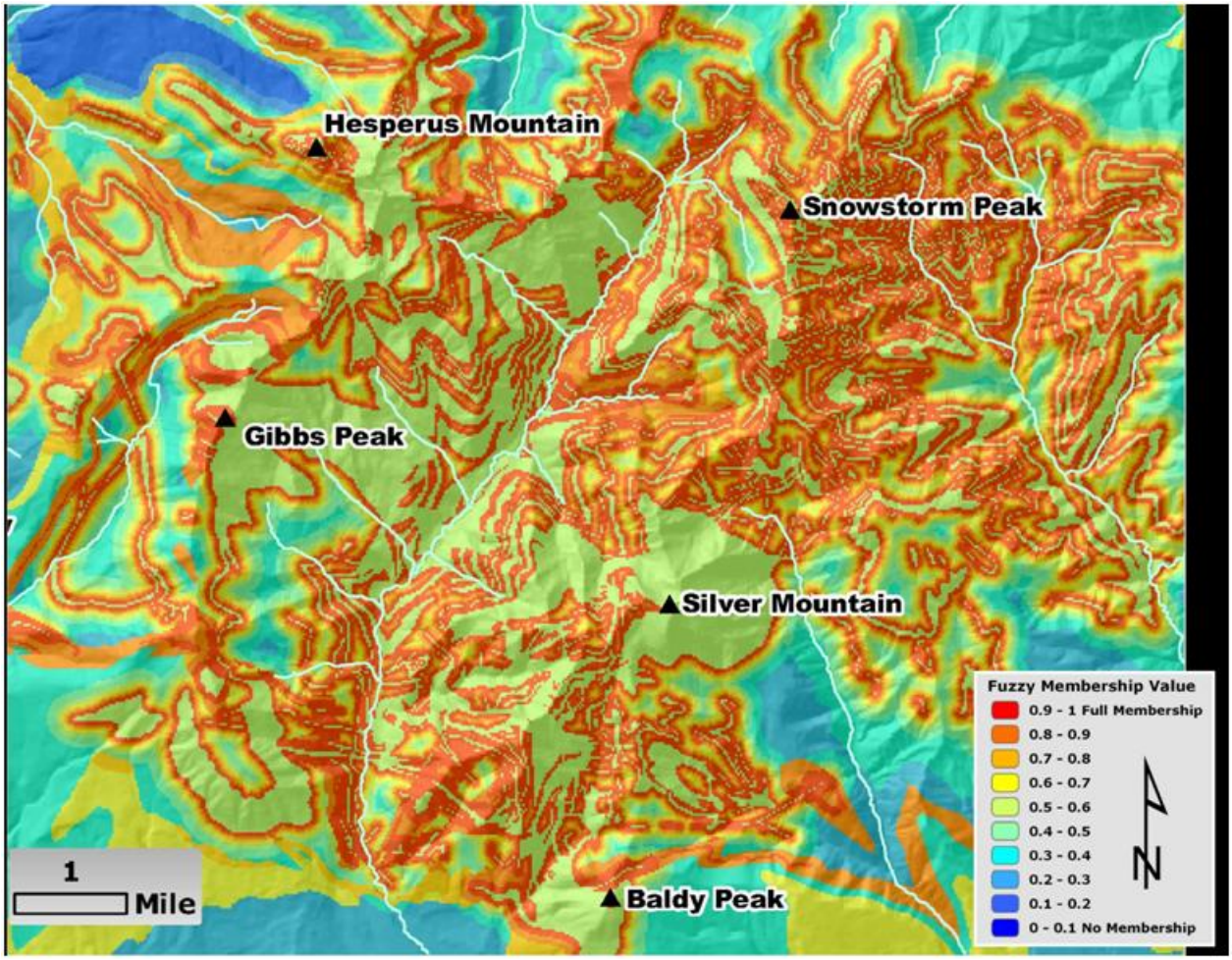

Figure 12. Lithological evidence map.

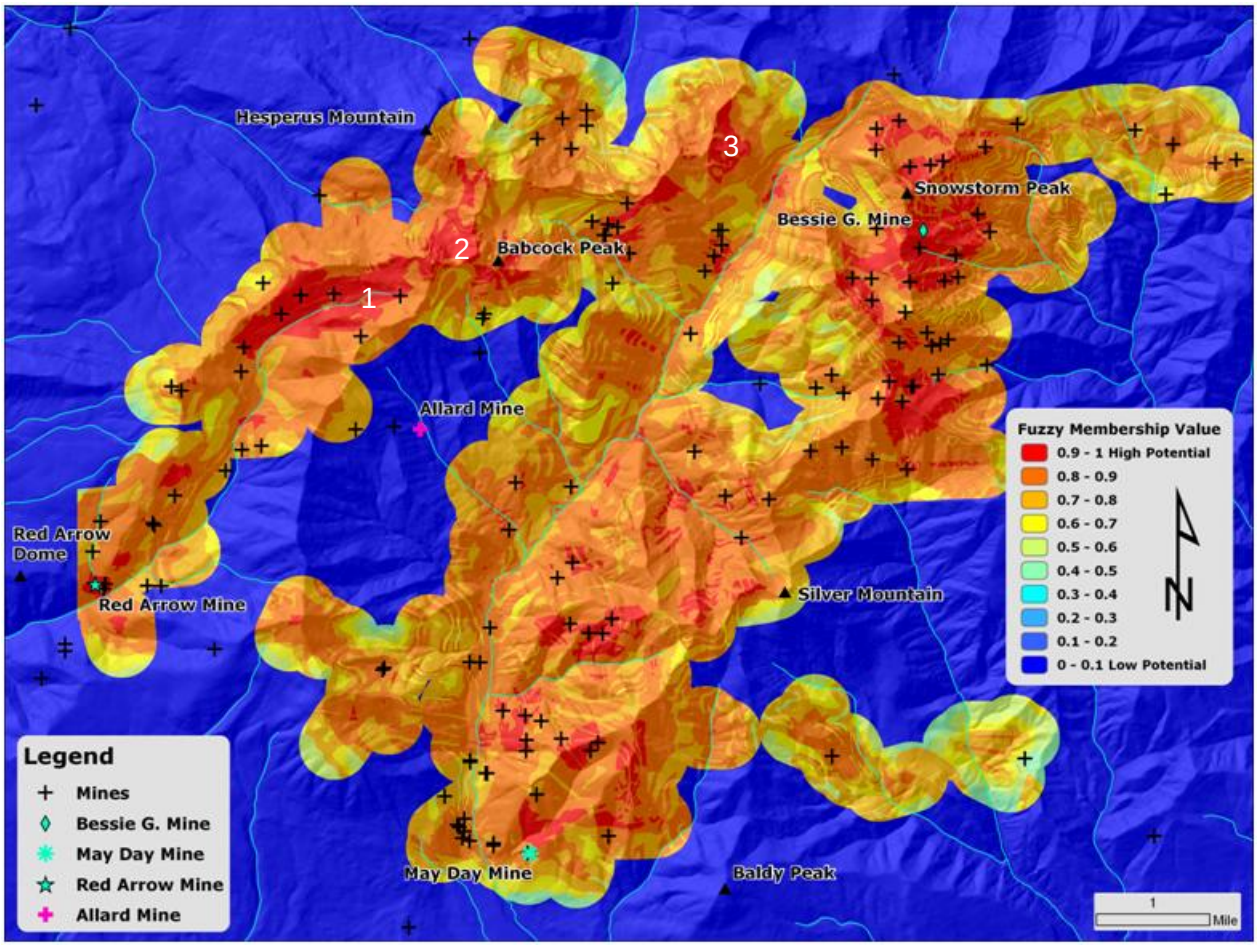

Figure 13. Gold potential map using a gamma of 0.95. Areas in red represent a high potential for gold mineralization, and areas in blue represent a low potential for gold mineralization. The Red Arrow Mine, May Day Mine and Bessie G Mine were correlated to areas with fuzzy membership values ≥ 0.9. White numbers indicate areas for further exploration.

Spatial Model Results

The spatial distribution of mines was compared to fuzzy membership values in the gold potential grid; the results of this comparison are summarized in Table 5. The upper East Mancos River had the most area with membership values ≥ 0.9. Overall, the model predicated 37 of the 158 total gold mines in study area to fuzzy membership values ≥ 0.9 (Table 5, Figure 13).

Table 5. Summary of Spatial Model Results						
	Area (km²)	**Percent**	**Areas ≥ 0.4***	**Mines**	**% Mines**	**% Mines in Areas ≥ 0.4***
Total	249			158		
Areas < 0.4*	147	59%		22	14%	
Areas ≥ 0.4*	102	41%	100%	136	86%	100%
Areas ≥ 0.8*	59	24%	58%	104	66%	76%
Areas ≥ 0.9*	9	4%	9%	37	23%	27%
*** Note that these numbers correspond to fuzzy membership values**						

Discussion of Results

Geochemical data acquired using the active stream sediment sampling technique indicates that the La Plata Mountains have elevated gold concentrations (Figure 7). A total of 29 basins have gold concentration greater than 10 ppb (Figure 7), which suggests that the sampling locations never reached the outer extent of the alteration halo. This is supported with elevated base metal concentrations throughout the district. High concentrations of gold, silver and arsenic were detected on the East Mancos River. This epithermal signature occurs on the backside of a known copper deposit (Allard Stock), and might indicate localized mineralization related to the syenite intrusive pluton.

Major structures in the region are generally oriented east-west with subordinate north-south trending structures; however, it is the intersection of these structures that are more likely to host high concentrations of precious metals. Regions with high vein and fault density suggest there was a considerable amount of fracturing during the emplacement of the igneous intrusions. These high density areas provided ample conduits for fluid movement during mineralization. Therefore, the vein and fault density map (Figure 6) is a good indicator of heavily mineralized zones. An example of areas that have vein intersections, but do not have any mines are the ridges connecting Spiller Peak and Babcock Peak, and the ridge connecting Mount Moss and Diorite Peak (Figure 6).

Based on studies from Eckel (1949), Saunders and May (1986), Trauger (1968), and Werle and others (1984), structures play an important role during gold deposition in the district; therefore, structures were weighted heavier in the final prediction surface by using two different structural surfaces (distance from veins grid and a vein and fault density grid) (Figure 10). This structural bias is apparent because the model did not predict any gold mineralization in areas that were farther than 500 meters from a vein. Regions that were within 500 meters of a mapped vein had fuzzy membership values ≥ 0.4 and this accounted for 86% of the known gold mines. This

supports previous studies' observations that structures were significant in gold deposition. Therefore, the qualities (location and identification) of mapped structures were the limiting factor in predicting gold mineralization within the district.

The fuzzy logic method allows for an integrated approach to modeling complex relationships among geochemical, structure and geologic datasets. The spatial model that was generated suggests several localities for further study. The model did a satisfactory job of locating deposits in areas that had a high density of mapped features and good geochemical coverage. The Bessie G, May Day and Red Arrow deposits were predicted with a fuzzy membership value ≥ 0.9 (Figure 13). The model indicates that 66% of known gold mines occur in areas with membership values ≥ 0.8 and 23% of known gold mines occur in regions with membership values ≥ 0.9. This signifies that in areas of good data coverage the model becomes a powerful predication tool; therefore, areas with no mines and fuzzy membership values ≥ 0.9 are good candidates for more detailed gold exploration and include: (1) the upper East Mancos River basin, (2) the South Fork of the West Mancos River basin, and (3) east of Diorite Peak (Figure 13).

Conclusion

Geochemical data of active stream sediment samples indicates that background concentrations of base and precious metals were not encountered in the 220 km² study area. There is a distinctive Au-As epithermal signature in the district and three major mines, the Bessie G., Red Arrow, and May Day were correlated to high fuzzy membership values ≥ 0.9. The East Mancos River basin contains the highest concentrations of Au (522 ppb high) and As (171 ppm high) in stream sediment.

The model considers that structures are a major controlling feature of gold ore deposition; therefore, it is limited by the quality and quantity of mapped structures. This is obvious in Figure 13, where data was clipped to the extent of the vein density buffer surface. These areas are clipped because any area that is not within 500 meters of a mapped vein was considered to have a membership value of zero. This is evident around the Allard Stock, where the model generated low membership values. The structural features used in this model were digitized from a geologic map produced in 1949. These structures were biased to gold deposits and did not map stockwork fracture sets common to most copper porphyry deposits like the Allard Stock.

Based on the model, areas that would be favorable for further gold exploration include: (1) the upper East Mancos River basin, (2) the South Fork of the West Mancos River basin, and (3) east of Diorite Peak (Figure 13).

References

Bonham-Carter, G. F., 1994, Geographic Information Systems for Geoscientists, Modelling with GIS, Pergamon, Ontario, pp. 290-301

Burrough, P.A., and McDonnel R.A., 1998, Principles of Geographical Information Systems, Oxford University Press, New York, pp 1-333.

Cross W. and Spencer C., 1899. Geologic Atlas of the United States: La Plata Folio, Colorado, Folio 60, USGS.

Eckel, E. B., 1936, Resurvey of the Geology and Ore Deposits of the La Plata Mining District, Colorado, Colorado Scientific Society, Denver Colorado, pp. 508-547.

Eckel, E. B., 1949, Geology and Ore Deposits of the La Plata district, Colorado: U.S. Geological Survey Professional Paper 219.

Lou, X., and Dimitrakopoulos, R., 2003, Data-driven fuzzy analysis in quantitative mineral assessment: Computers and Geosciences, Vol. 29, pp. 3-13.

Panteleyev, A., 1995, Porphyry Cu-Au (Alkalic); Selected British Columbia Mineral Deposit Profiles (27A, Economic geology, geology of ore deposits No. 1995-20). Canada.

Saunders, J. A. and May, E. R., 1986, Bessie G: A High Grade Epithermal Gold Telluride Deposit, La Plata County, Colorado, U.S.A., Proceedings of Gold ’86 Symposium, Toronto, pp. 436-444.

Sawatzky, D.L., Raines, G.L. , Bonham-Carter, G.F., and Looney, C.G., 2007, Spatial Data Modeller (SDM): ArcMAP 9.2 geoprocessing tools for spatial data modelling using weights of evidence, logistic regression, fuzzy logic and neural networks. *<http://arcscripts.esri.com/details.asp?dbid=15341.>*

Tsoukalas, L.H., and Uhrig, R.E., 1997, Fuzzy and neural approaches in engineering: New York, John Wiley and Sons, Inc., pp. 587.

Trauger, F.D., 1968, Geology and Ore Deposits of the La Plata District, Colorado, Digest of USGS Professional Paper 219, in San Juan – San Miguel – La Plata Region New Mexico and Colorado, New Mexico Geological Society 19th field conference.

U.S. Geological Survey, 2008, USGS Mineral Resources On-Line Spatial Data, Retreived on January 15, 2008, http://tin.er.usgs.gov/.

Werle, J. L., Ikramuddin, M., and Mutschler, F. E., 1984, Allard Stock, La Plata Mountains, Colorado; An alkaline rock-hosted porphyry copper - precious metal deposit, Canadian Journal of Earth Sciences, Vol. 21 No.6, pp. 630-641.

Acknowledgments

Funding for this project provided by Fort Lewis College Student Research Grant (Summer 2007 and Winter 2008). This paper represents a modified version of the primary author's senior thesis at Fort Lewis College, Department of Geosciences, advised by Jeff Cary and Dr. Scott White. For a complete copy of the paper, including the geologic map of the La Plata Mountains, contact the primary author, David Schiowitz (david@bikiswater.com).

Special thanks to Bob Schiowitz, Matt Clement, Jack Blaisdell, Travis Bearden, Jon Moore, Clint Holnback, and Wade Johnston for helping with geochemical sample collection, American Assay Laboratories for analyzing the stream sediment samples, and Dr. Gary Raines for answering questions about the Spatial Data Modeller GIS extension.